Supporting Information for

Atomistic Design of Microbial Opsin-based Blue-Shifted Optogenetics Tools

Authors: Hideaki E. Kato[1†*], Motoshi Kamiya[2*], Seiya Sugo[2], Jumpei Ito[3], Reiya Taniguchi[1], Ayaka Orito[3], Kunio Hirata[4], Ayumu Inutsuka[5], Akihiro Yamanaka[5], Andrés D. Maturana[3], Ryuichiro Ishitani[1], Yuki Sudo[6], Shigehiko Hayashi[2**], and Osamu Nureki[1**]

Affiliations: *[1]Department of Biological Sciences, Graduate School of Science, The University of Tokyo, 2-11-16 Yayoi, Bunkyo-ku, Tokyo 113-0032, Japan; [2]Department of Chemistry, Graduate School of Science, Kyoto University, Kyoto 606-8502, Japan; [3]Department of Bioengineering Sciences, Graduate School of Bioagricultural Sciences, Nagoya University, Furo-cho, Chikusa-ku, Nagoya 464-8601, Japan; [4]RIKEN SPring-8 Center, Hyogo 679-5148, Japan; [5]Department of Neuroscience II, Research Institute of Environmental Medicine, Nagoya University, Nagoya 464-8601, Japan; [6]Division of Pharmaceutical Sciences, Graduate School of Medicine, Dentistry, and Pharmaceutical Sciences, Okayama University, 1-1-1 Tsushima-naka, Kita-ku, Okayama 700-8530, Japan.*

†Present address: Department of Molecular and Cellular Physiology, Stanford University School of

Medicine, Stanford, California 94305, USA.

**Corresponding author. E-mail: hayashig@kuchem.kyoto-u.ac.jp (S.H.); nureki@bs.s.u-tokyo.ac.jp (O.N.)*

Figure Captions for Supplementary figures

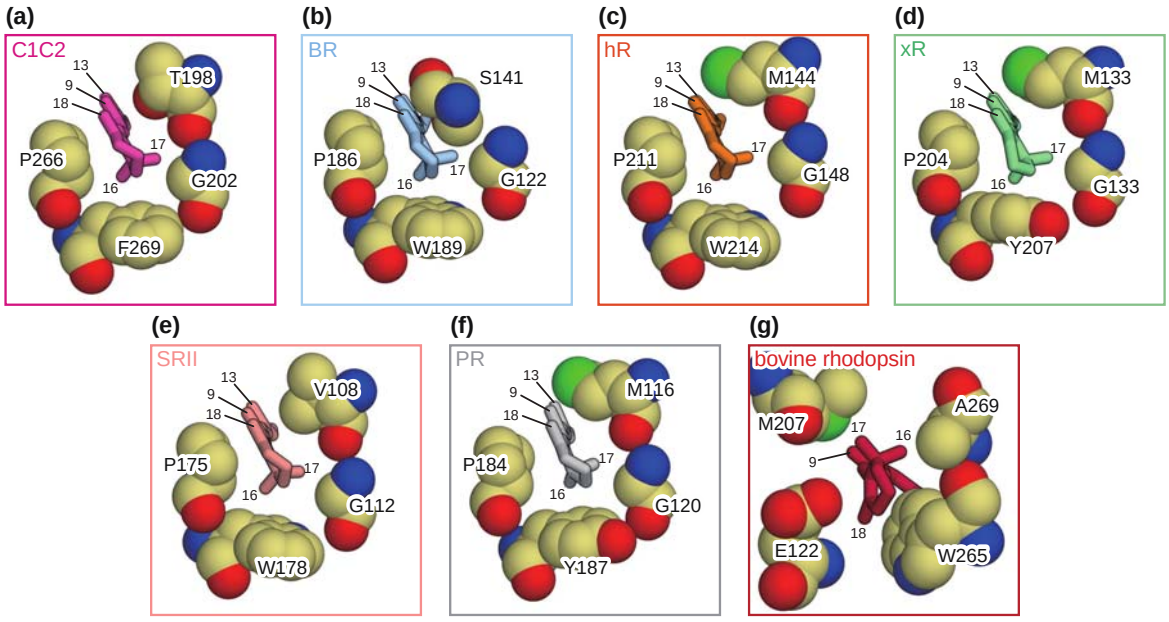

Supplementary Figure 1: Comparison of the retinal binding pockets. The retinal binding pockets of C1C2WT (a), BR (b), halorhodopsin (hR) (c), xanthorhodopsin (xR) (d), SRII (e), PR (f), and bovine rhodopsin (g). Retinal molecules are depicted by stick models, and the surrounding residues are shown as cpk models.

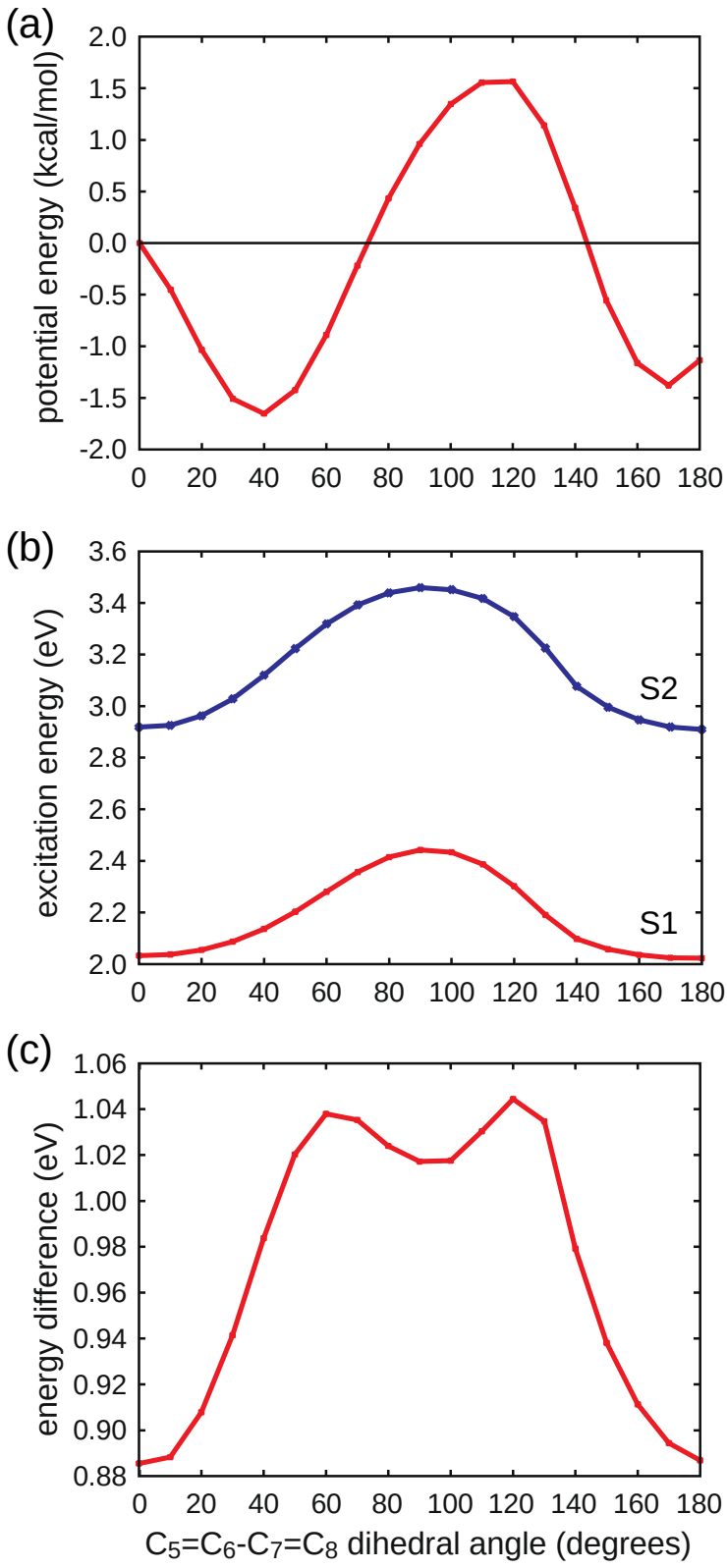
(a)
potential energy (kcal/mol)
2.0
1.5
1.0
0.5
0.0
-0.5
-1.0
-1.5
-2.0
0
20
40
60
80
100
120
140
160
180
(b)
excitation energy (eV)
3.6
3.4
3.2
3.0
2.8
2.6
2.4
2.2
2.0
S2
S1
(c)
energy difference (eV)
1.06
1.04
1.02
1.00
0.98
0.96
0.94
0.92
0.90
0.88
C5=C6-C7=C8 dihedral angle (degrees)

Supplementary Figure 2: Potential energy and excitation energies of RPSB with torsion around the C_6-C_7 bond in the gas phase. The ground (S_0) state geometries of the isolated RPSB moiety, which is the QM region of the QM/MM system of C1C2, along the torsional coordinate were optimized at the M06-2X/6-31G** level of theory. (a) Potential energy curve of the ground state (M06-2X/6-31G**). (b) Changes of the S_1 and S_2 excitation energies of RPSB. The excitation energies were calculated with the second order extended multi-configuration quasi-degenerate perturbed theory (XMCQDPT2) level of theory with a three-state averaged density, where all the valence π-orbitals and π-electrons of RPSB were involved in the active space and electrons, respectively. Basis functions of 6-31G** were employed for the XMCQDPT2 calculations. (c) Change in the S_1-S_2 energy difference.

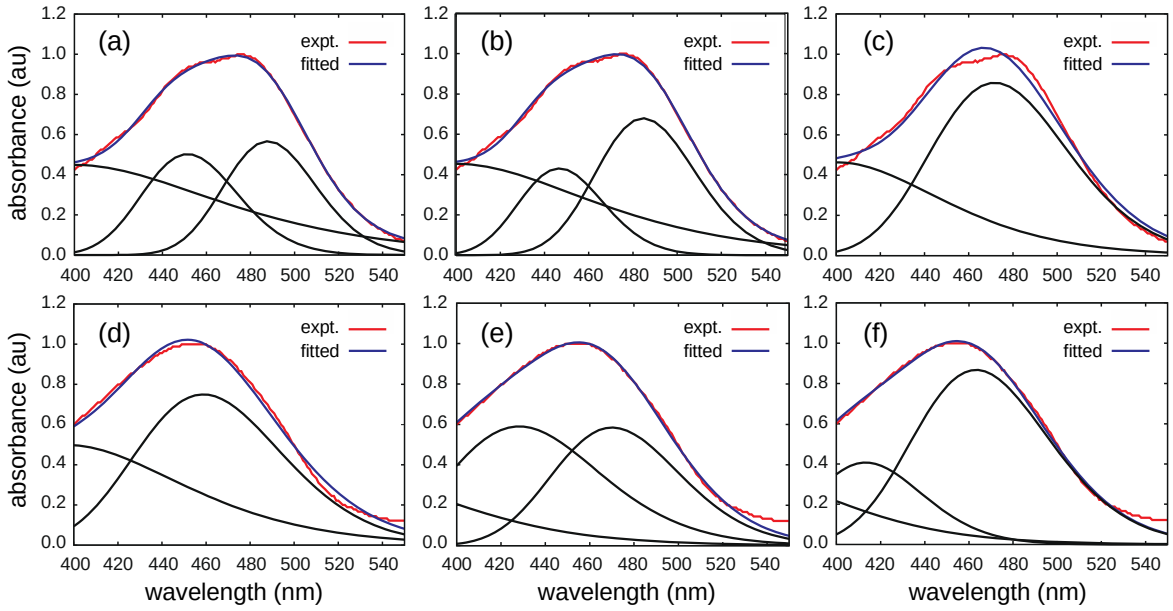

Supplementary Figure 3: Decomposition of absorption spectra of C1C2WT and C1C2GA into spectral components expressed by Gaussian functions. Fitted parameters are listed in Supplementary Table 3. Red and blue curves indicate experimental absorption spectra (expt.) and fitted ones (fitted), respectively. Black curves are Gaussian components determined by the fitting. (a) C1C2WT fitted with three Gaussian functions, (b) C1C2WT fitted with three Gaussian functions assuming the same widths for the main and shoulder peaks, (c) C1C2WT fitted with two Gaussian functions, (d) C1C2GA fitted with two Gaussian functions, (e) C1C2GA fitted with three Gaussian functions, and (f) C1C2GA fitted with three Gaussian functions assuming the same widths for two peaks. The absorption spectrum of C1C2WT fit well with three Gaussian functions (a,b). Two sharp Gaussian functions express the main peak and the shoulder peak, respectively, and one broad one at ~72 kcal/mol (Supplementary Table 3) represents a component of the denatured state. In contrast, the absorption spectrum of C1C2WT obviously cannot be expressed with two Gaussian functions (c), indicating that two components are necessary to represent the fine structures of the main band. The absorption spectrum of C1C2GA is well expressed with two Gaussian functions with a consistent component of the denatured state at 72 kcal/mol (Supplementary Table 3) (d), whereas the spectrum failed to be consistently fitted with three Gaussian functions (e,f); components of the denatured state are found at ~80 kcal/mol and are inconsistent with the other fittings. One component is therefore sufficient to represent the main band of C1C2GA.

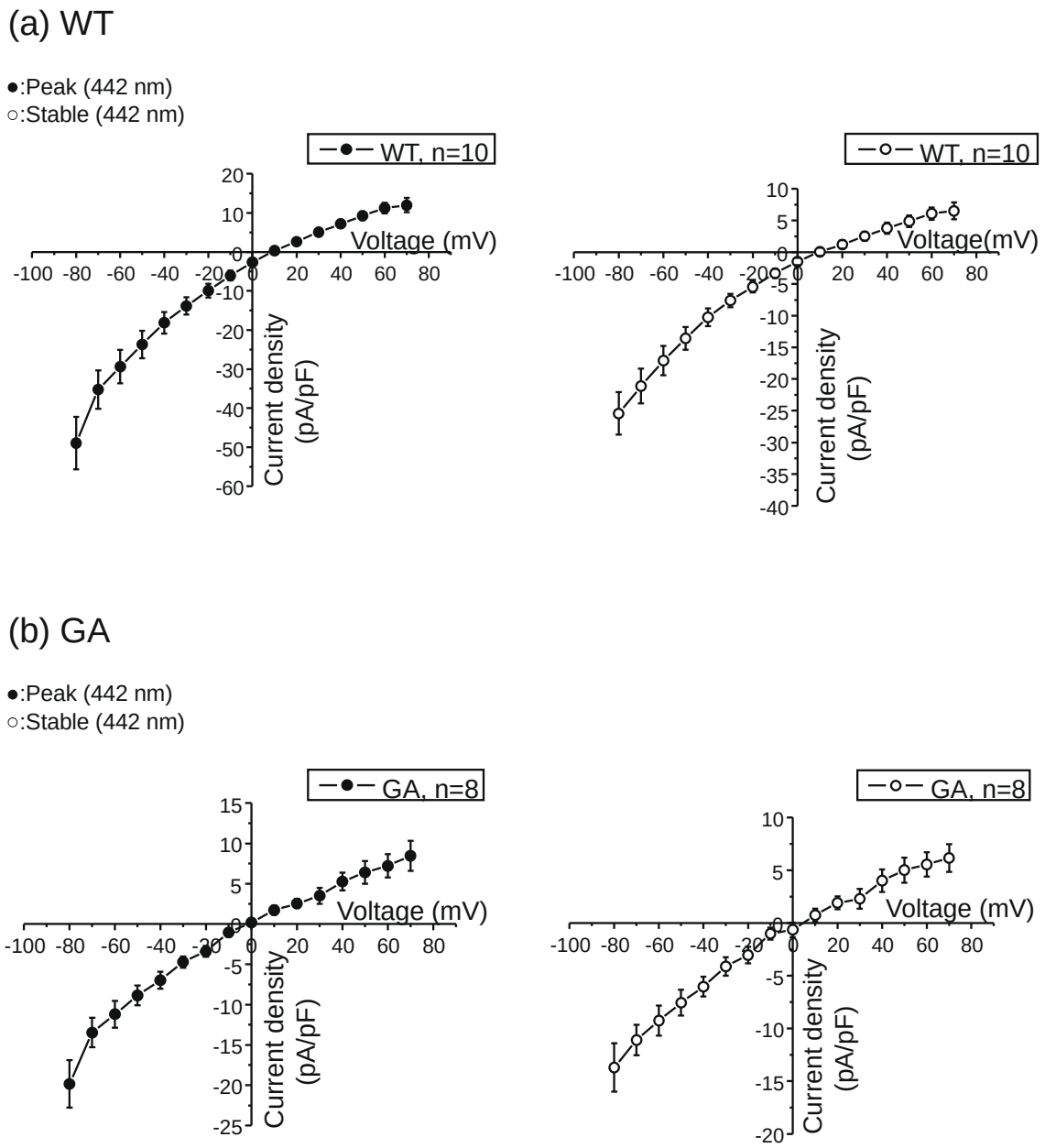

Supplementary Figure 4: Current-voltage (I-V) curves of C1C2WT (a) and the C1C2GA mutant (b). The I-V relationships between -80 and + 70mV were determined from the single current amplitude at the indicated potentials. Values are means and SEM of 8-10 experiments.

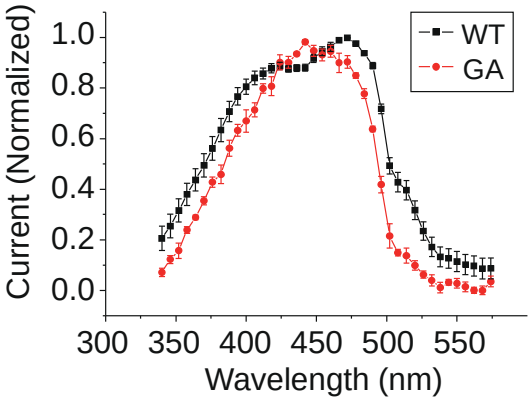

Supplementary Figure 5: Action spectra of C1C2WT (black) and C1C2GA (red). Each spectrum is normalized to its own peak for ease of comparison. In the action spectrum of C1C2WT, a second peak at 420 nm appears, in addition to the first peak at 470 nm. Note that the band corresponding to the second peak is absent in the absorption spectrum; the second peak in the action spectrum is located at a significantly shorter wavelength than the sub-band in the absorption maximum (450 nm). The absence of the corresponding peak in the absorption spectrum indicates that the photocurrent at the second peak in the action spectrum does not originate from a state in the resting dark state. From a structural point of view, the binding of the retinal chromophore in the 6-*s*-*cis* conformation in the binding pocket of the wild-type is also unlikely. A likely explanation would be a second conducting state in a branch of the photocycle.

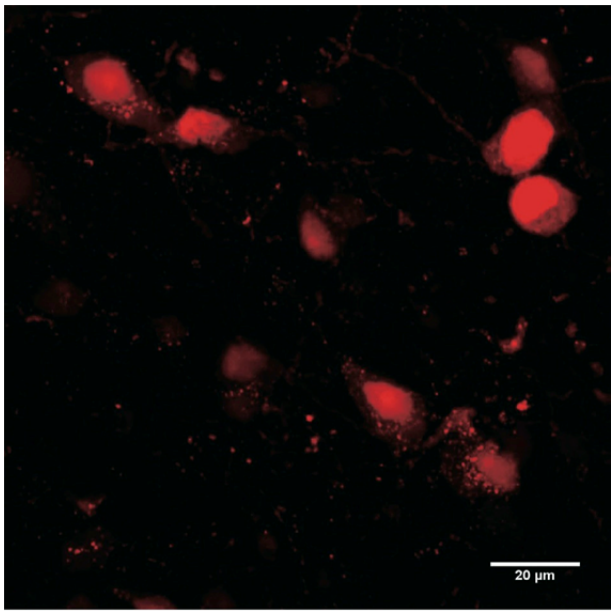

Supplementary Figure 6: EGFP-fused C1C2GA expression in neurons. Confocal image of representative mouse neurons expressing C1C2GA. Scale bar represents 20 µm.

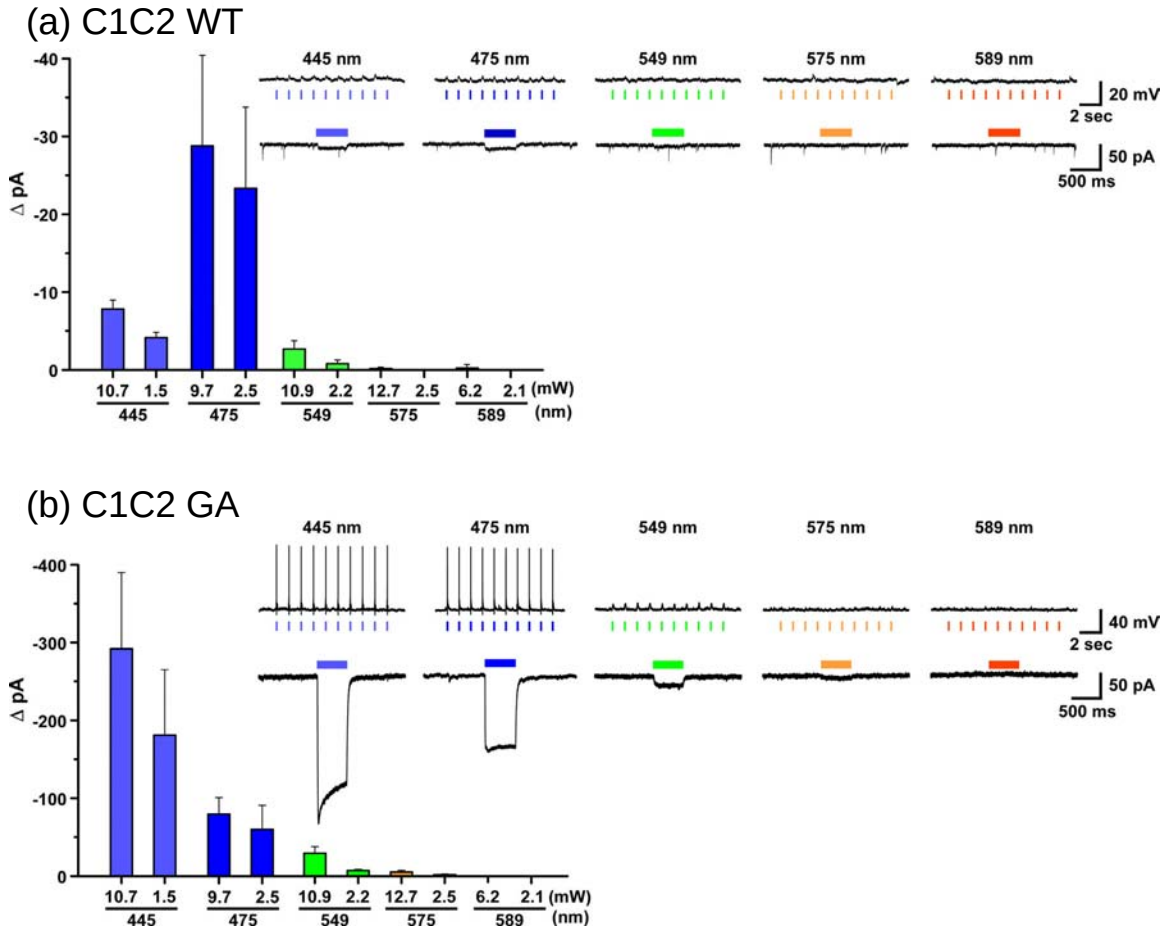

Supplementary Figure 7: Channel properties of C1C2WT (a) and C1C2GA (b) in mouse neurons. Peak amplitudes, current-clamp mode recordings, and photocurrents using light pulses at different wavelengths (100 ms, 1-2 Hz) are shown.

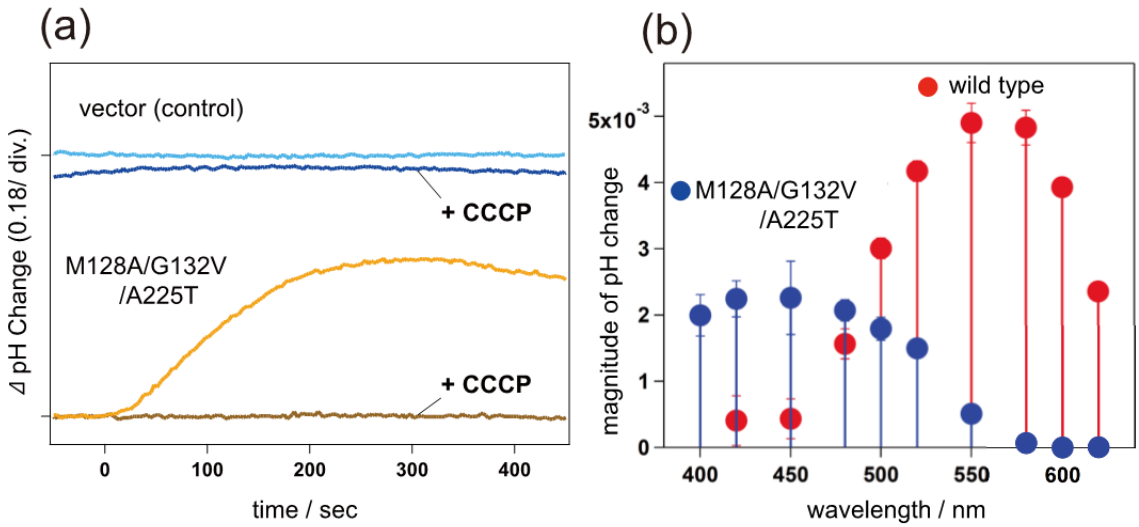

Supplementary Figure 8: (a) Light-induced pH change by H^+-transport by the M128A/G132V/A225T mutant of AR3. The suspension of *E. coli* carrying only the vector (pBAD24) did not show any pH change upon light illumination. The pH change induced by the M128A/G132V/A225T mutation was cancelled by the addition of a protonophore (CCCP). The light illumination ($\lambda > 430$ nm) began at $t = 0$ s and ceased at $t = 150$ s. (b) Action spectra for the proton pumping activity in transformants containing the wild type (red circles) or the M128A/G132V/A225T mutant (blue circles) of AR3, which were estimated from the initial slopes of the pH change. The error bars indicate the standard deviations of three identical experiments.

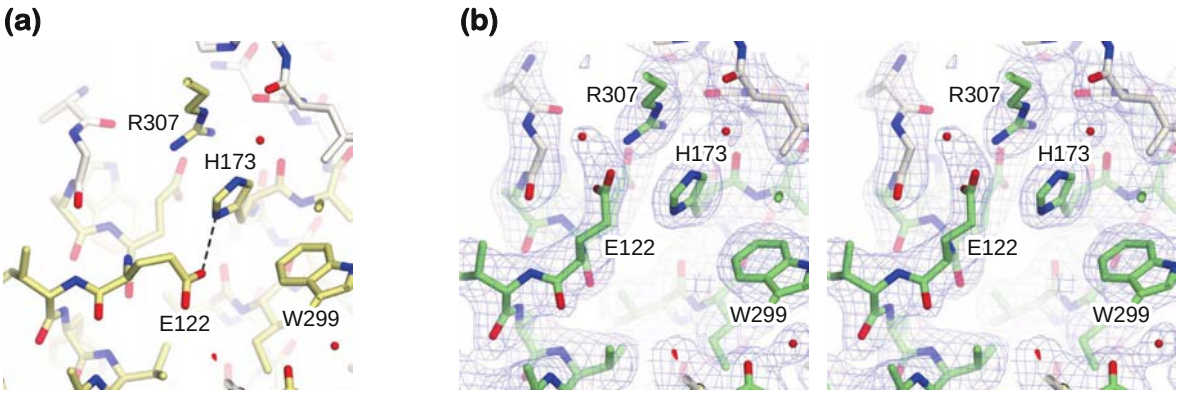

Supplementary Figure 9: Structural comparison around the intracellular channel gate between C1C2WT and C1C2GA. (a) The C1C2WT structure around Glu122. (b) Stereo view of the C1C2GA structure in the same region. The 2Fo-Fc map (blue mesh, contoured at 1.0 σ) is shown. Water molecules are shown as red spheres, and the hydrogen bond is represented by the black dashed line.

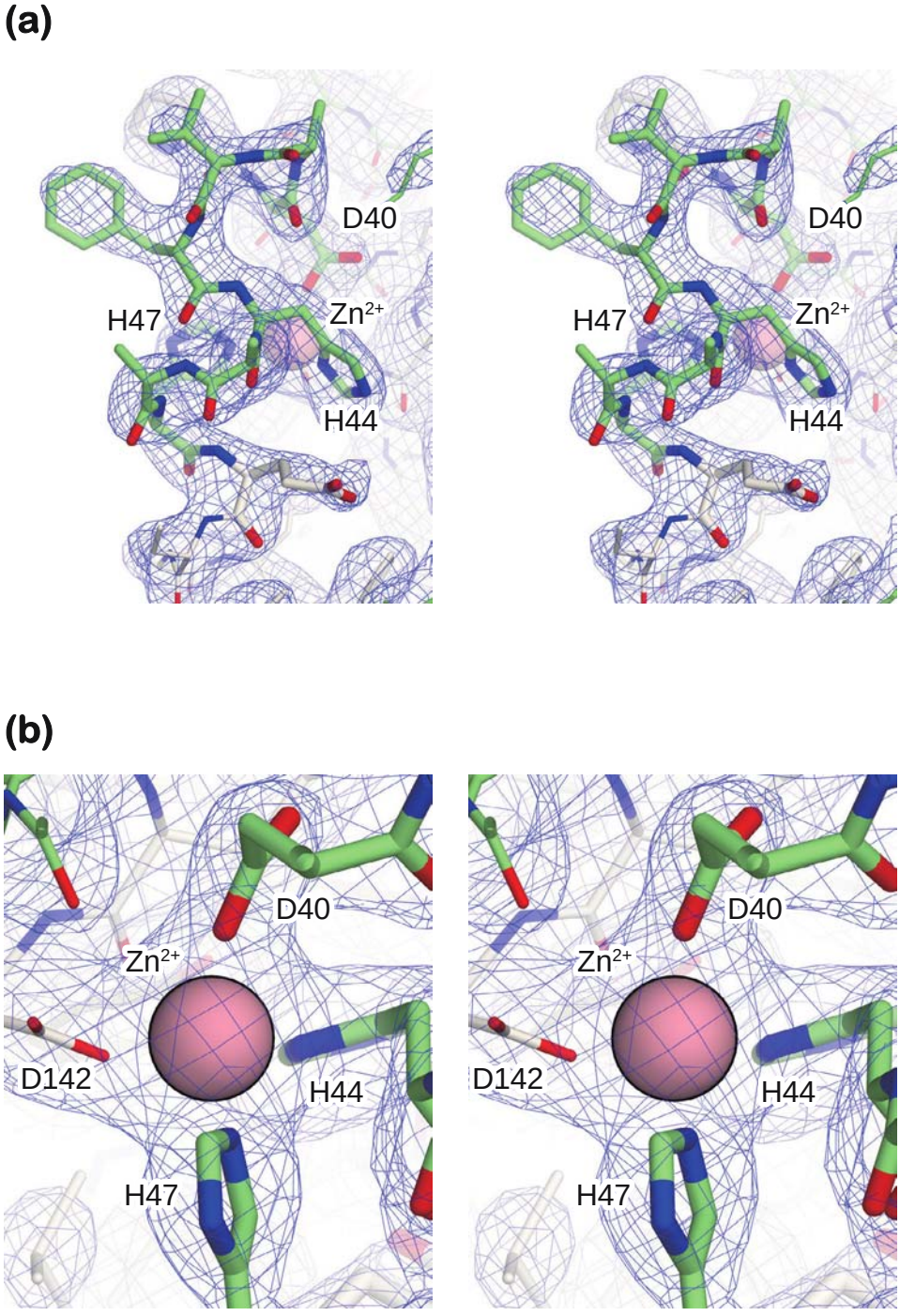

Supplementary Figure 10: Electron densities around the N-terminal region and the putative Zn^{2+} binding site. Stereo views of the structures and densities in the overall N-terminal region (a) and the Zn^{2+}binding site (b). Zn^{2+} is shown as a cpk model, and the N-terminal 10 residues (PDAVFHRAHE)

are represented as thicker stick models. The $2F_o$-F_c maps (blue mesh, contoured at 1.0 σ) are shown.

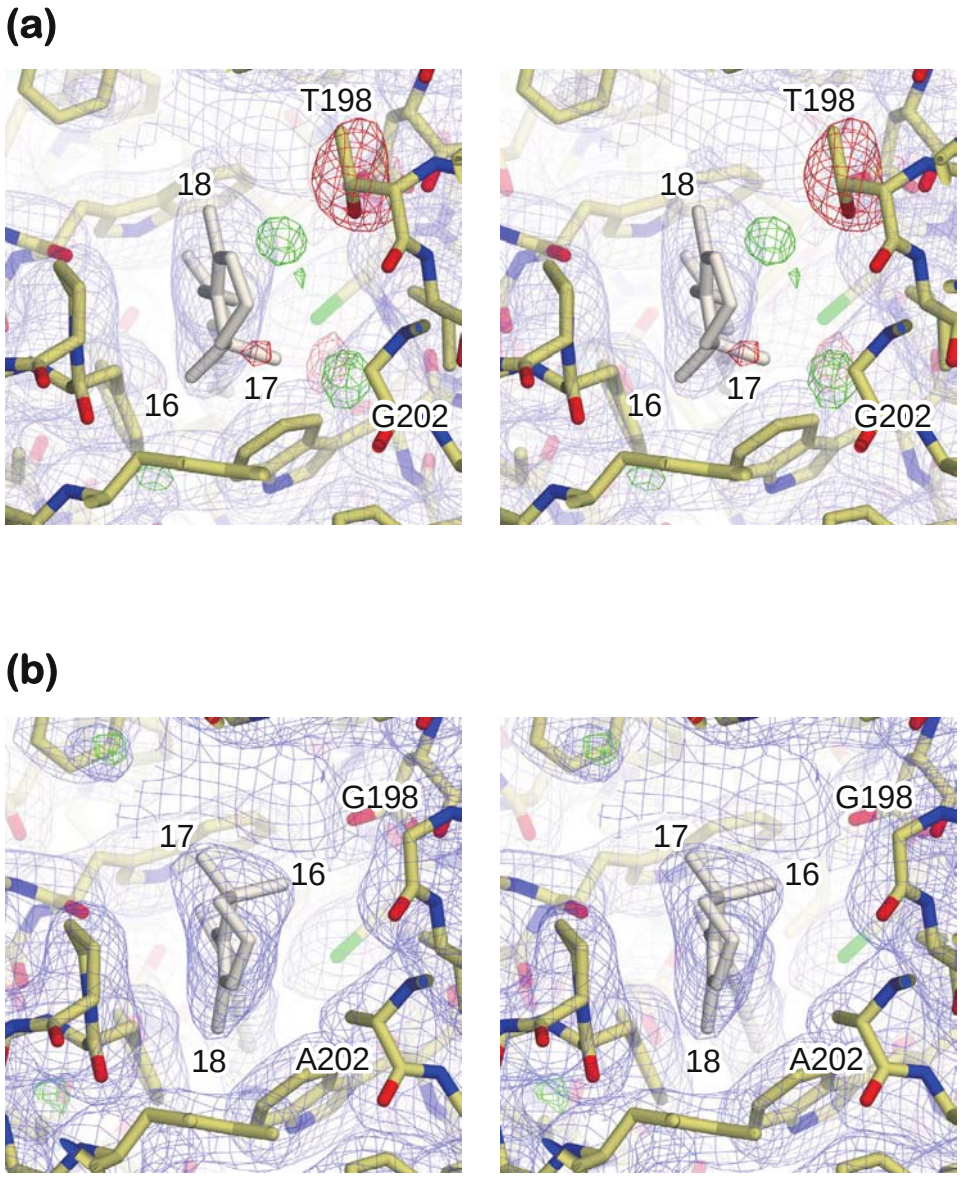

Supplementary Figure 11: Electron density maps around the β-ionone ring in the C1C2GA mutant. (a) Stereo views of the structures and densities around the β-ionone ring, just after the molecular replacement using the C1C2WT structure (PDB ID: 3UG9). The $2F_o$-F_c map (blue mesh, contoured at 1.0 σ) and the F_o-F_c map (green and red meshes, contoured at 3.0 and -3.0 σ, respectively) are shown. The negative peak at C_{17} and the positive peak between C_{18} and T198 in the F_o-F_c map clearly indicate that the β-ionone ring of this mutant is rotated, as compared to that of C1C2 WT. (b) Stereo views of the structures and densities around the β-ionone ring after the structural refinement. The $2F_o$-F_c map (blue

mesh, contoured at 1.0 σ) and the F_o-F_c map (green and red meshes, contoured at 3.0 and -3.0 σ, respectively) are shown. This F_o-F_c map without any strong negative or positive peak around the β-ionone ring demonstrates that the β-ionone ring of the retinal molecule in C1C2GA mutant is significantly rotated, and the retinal configuration changes from 6-*s*-*trans* to 6-*s*-*cis*.

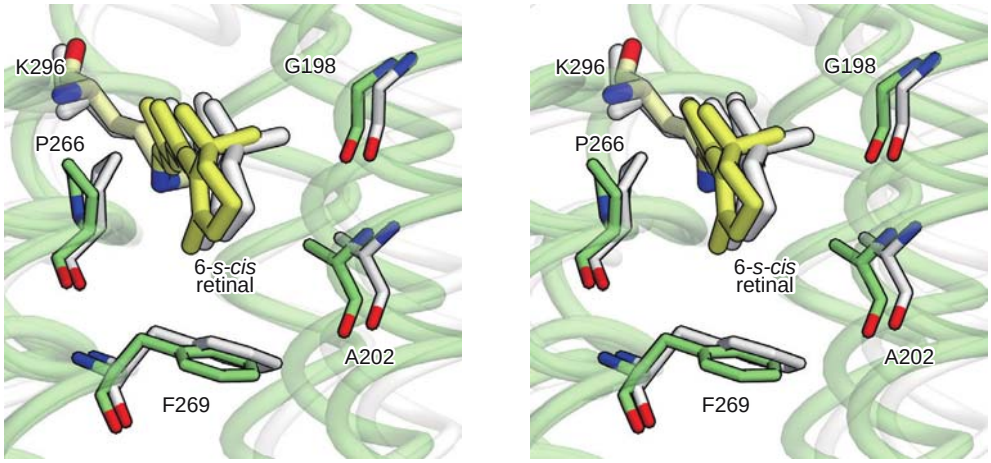

Supplementary Figure 12: Structural comparison of the retinal and its binding pocket between the X-ray structure (green) and the calculated model (grey). Retinal molecules are colored yellow (X-ray) and grey (calculated model).

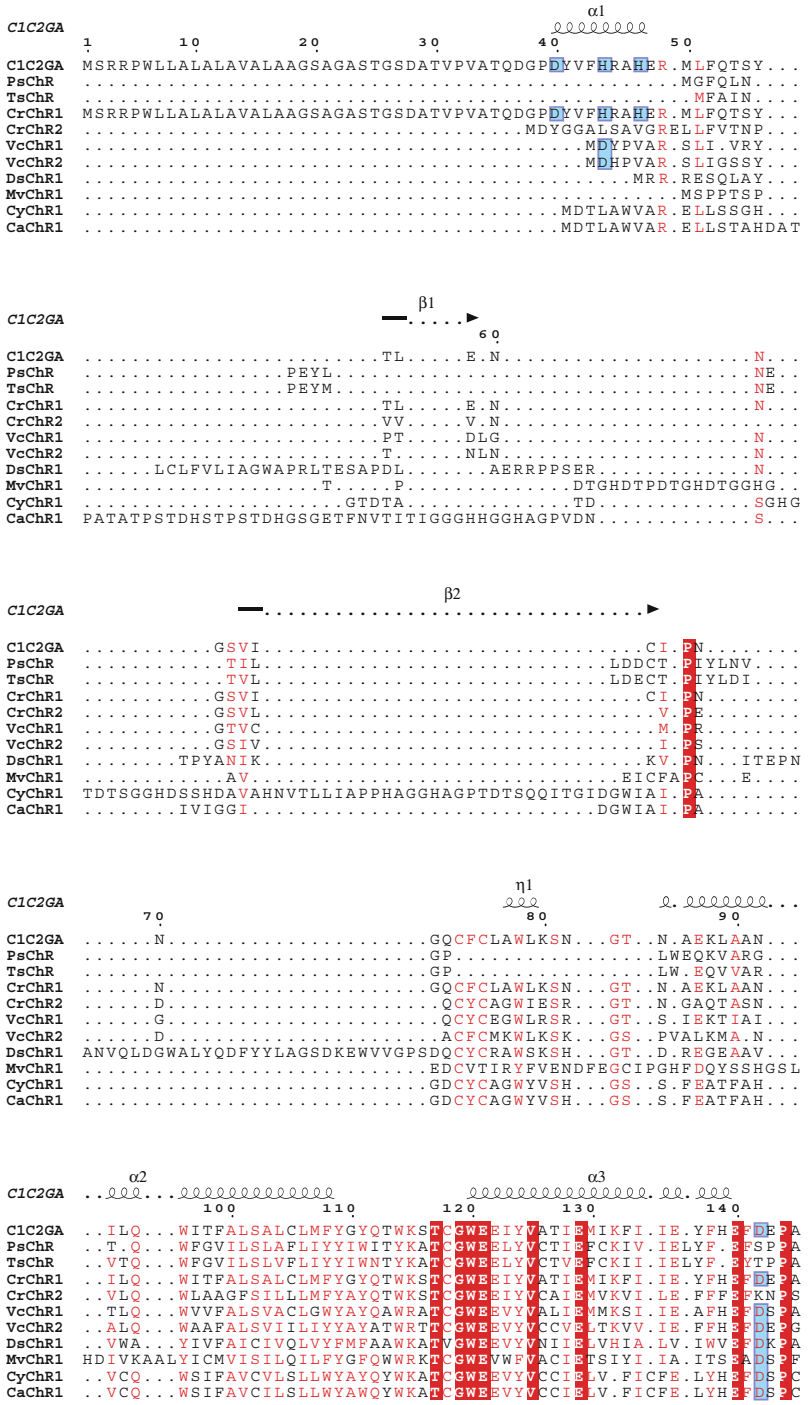
α1
β1
β2
η1
α2
α3
C1C2GA
C1C2GA MSRRPWLLALALAVALAAGSAGASTGSDATVPVATQDGPDYVFHRAHER.MLFQTSY...
PsChR .....MGFQLN....
TsChR .....MFAIN....
CrChR1 MSRRPWLLALALAVALAAGSAGASTGSDATVPVATQDGPDYVFHRAHER.MLFQTSY...
CrChR2 .....MDYGGALSAVGRELLFVTNP...
VcChR1 .....MDYPVAR.SLI.VRY...
VcChR2 .....MDHPVAR.SLIGSSY...
DsChR1 .....MRR.RESQLAY...
MvChR1 .....MSPPTSP...
CyChR1 .....MDTLAWVAR.ELLSSGH...
CaChR1 .....MDTLAWVAR.ELLSTAHDAT
C1C2GA .....TL.....E.N.....N...
PsChR .....PEYL.....NE..
TsChR .....PEYM.....NE..
CrChR1 .....TL.....E.N.....N...
CrChR2 .....VV.....V.N.....
VcChR1 .....PT.....DLG.....N...
VcChR2 .....T.....NLN.....N...
DsChR1 .....LCLFVLIAGWAPRLTESAPDL.....AERRPPSER.....N...
MvChR1 .....T.....P.....DTGHDTPDTGHDTGGHG..
CyChR1 .....GTDTA.....TD.....SGHG
CaChR1 PATATPSTDHSTPSTDHGSGETFNVTITIGGGHHGGHAGPVDN.....S...
C1C2GA .....GSVI.....CI.PN.....
PsChR .....TIL.....LDDCT.PIYLNV....
TsChR .....TVL.....LDECT.PIYLDI....
CrChR1 .....GSVI.....CI.PN.....
CrChR2 .....GSVL.....V.PE.....
VcChR1 .....GTVC.....M.PR.....
VcChR2 .....GSIV.....I.PS.....
DsChR1 .....TPYANIK.....KV.PN...ITEPN
MvChR1 .....AV.....EICFAPC...E....
CyChR1 TDTSGGHDSSHDAVAHNVTLLIAPPHAGGHAGPTDTSQQITGIDGWIAI.PA.....
CaChR1 .....IVIGGI.....DGWIAI.PA.....
C1C2GA .....N.....GQCFCLAWLKSN...GT..N.AEKLAAN...
PsChR .....GP.....LWEQKVARG...
TsChR .....GP.....LW.EQVVAR...
CrChR1 .....N.....GQCFCLAWLKSN...GT..N.AEKLAAN...
CrChR2 .....D.....QCYCAGWIESR...GT..N.GAQTASN...
VcChR1 .....G.....QCYCEGWLRSR...GT..S.IEKTIAI...
VcChR2 .....D.....ACFCMKWLKSK...GS..PVALKMA.N...
DsChR1 ANVQLDGWALYQDFYYLAGSDKEWVVGPSDQCYCRAWSKSH...GT..D.REGEAAV...
MvChR1 .....EDCVTIRYFVENDFEGCIPGHFDQYSSHGSL
CyChR1 .....GDCYCAGWYVSH...GS..S.FEATFAH...
CaChR1 .....GDCYCAGWYVSH...GS..S.FEATFAH...
C1C2GA ..ILQ...WITFALSALCLMFYGYQTWKSTCGWEEIYVATIEMIKFI.IE.YFHEFDEPA
PsChR ..T.Q...WFGVILSLAFLIYYIWITYKATCGWEELYVCTIEFCKIV.IELYF.EFSPPA
TsChR ..VTQ...WFGVILSLVFLIYYIWNTYKATCGWEELYVCTVEFCKII.IELYF.EYTPPA
CrChR1 ..ILQ...WITFALSALCLMFYGYQTWKSTCGWEEIYVATIEMIKFI.IE.YFHEFDEPA
CrChR2 ..VLQ...WLAAGFSILLLMFYAYQTWKSTCGWEEIYVCAIEMVKVI.LE.FFFEFKNPS
VcChR1 ..TLQ...WVVFALSVACLGWYAYQAWRATCGWEEVYVALIEMMKSI.IE.AFHEFDSPA
VcChR2 ..ALQ...WAAFALSVIILIYYAYATWRTTCGWEEVYVCCVELTKVV.IE.FFHEFDEPG
DsChR1 ..VWA...YIVFAICIVQLVYFMFAAWKATVGWEEVYVNIIELVHIA.LV.IWVEFDKPA
MvChR1 HDIVKAALYICMVISILQILFYGFQWWRKTCGWEVWFVACIETSIYI.IA.ITSEADSPF
CyChR1 ..VCQ...WSIFAVCVLSLLWYAYQYWKATCGWEEVYVCCIELV.FICFE.LYHEFDSPC
CaChR1 ..VCQ...WSIFAVCILSLLWYAWQYWKATCGWEEVYVCCIELV.FICFE.LYHEFDSPC

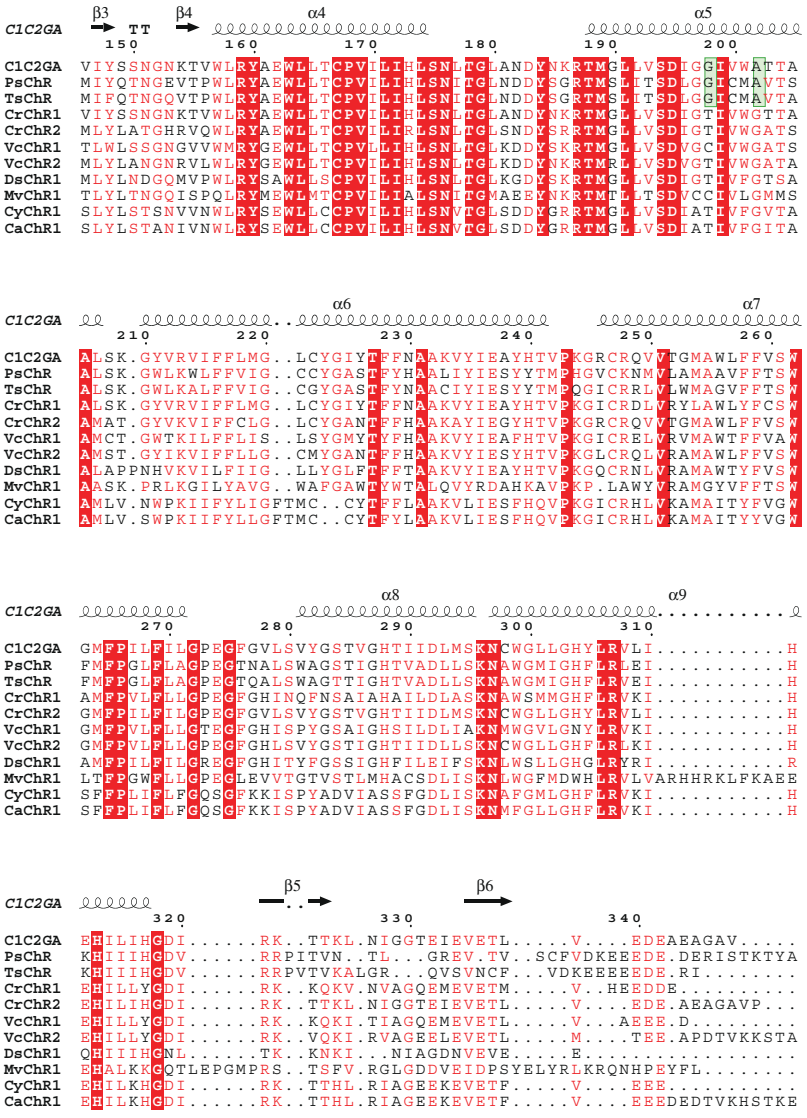
β3
β4
α4
α5
C1C2GA
150
160
170
180
190
200
C1C2GA VIYSSNGNKTVWLRYAEWLLTCPVILIHLSNLTGLANDYNKRTMGLLVSDIGGIVWATTA
PsChR MIYQTNGEVTPWLRYAEWLLTCPVILIHLSNITGLNDDYSGRTMSLITSDLGGICMAVTS
TsChR MIFQTNGQVTPWLRYAEWLLTCPVILIHLSNITGLNDDYSGRTMSLITSDLGGICMAVTA
CrChR1 VIYSSNGNKTVWLRYAEWLLTCPVILIHLSNLTGLANDYNKRTMGLLVSDIGTIVWGTTA
CrChR2 MLYLATGHRVQWLRYAEWLLTCPVILIRLSNLTGLSNDYSRRTMGLLVSDIGTIVWGATS
VcChR1 TLWLSSGNGVVWMRYGEWLLTCPVLLIHLSNLTGLKDDYSKRTMGLLVSDVGCIVWGATS
VcChR2 MLYLANGNRVLWLRYGEWLLTCPVILIHLSNLTGLKDDYNKRTMRLLVSDVGTIVWGATA
DsChR1 MLYLNDGQMVPWLRYSAWLLSCPVILIHLSNLTGLKGDYSKRTMGLLVSDIGTIVFGTSA
MvChR1 TLYLTNGQISPQLRYMEWLMTCPVILIAWSNITGMAEEYNKRTMTLLTSDVCCIVLGMMS
CyChR1 SLYLSTSNVVNWLRYSEWLLCCPVILIHLSNVTGLSDDYGRRTMGLLVSDIATIVFGVTA
CaChR1 SLYLSTANIVNWLRYSEWLLCCPVILIHLSNVTGLSDDYGRRTMGLLVSDIATIVFGITA
α6
α7
C1C2GA
210
220
230
240
250
260
C1C2GA ALSK.GYVRVIFFLMG..LCYGIYTFFNAAKVYIEAYHTVPKGRCRQVVTGMAWLFFVSW
PsChR ALSK.GWLKWLFFVIG..CCYGASTFYHAALIYIESYYTMPHGVCKNMVLAMAAVFFTSW
TsChR ALSK.GWLKALFFVIG..CGYGASTFYNAACIYIESYYTMPQGICRRLVLWMAGVFFTSW
CrChR1 ALSK.GYVRVIFFLMG..LCYGIYTFFNAAKVYIEAYHTVPKGICRDLVRYLAWLYFCSW
CrChR2 AMAT.GYVKVIFFCLG..LCYGANTFFHAAKAYIEGYHTVPKGRCRQVVTGMAWLFFVSW
VcChR1 AMCT.GWTKILFFLIS..LSYGMYTYFHAAKVYIEAFHTVPKGICRELVRVMAWTFFVAW
VcChR2 AMST.GYIKVIFFLLG..CMYGANTFFHAAKVYIESYHTVPKGLCRQLVRAMAWLFFVSW
DsChR1 ALAPPNHVKVILFIIG..LLYGLFTFFTAAKVYIEAYHTVPKGQCRNLVRAMAWTYFVSW
MvChR1 AASK.PRLKGILYAVG..WAFGAWTYWTALQVYRDAHKAVPKP.LAWYVRAMGYVFFTSW
CyChR1 AMLV.NWPKIIFYLIGFTMC..CYTFFLAAKVLIESFHQVPKGICRHLVKAMAITYFVGW
CaChR1 AMLV.SWPKIIFYLLGFTMC..CYTFYLAAKVLIESFHQVPKGICRHLVKAMAITYYVGW
α8
α9
C1C2GA
270
280
290
300
310
C1C2GA GMFPILFILGPEGFGVLSVYGSTVGHTIIDLMSKNCWGLLGHYLRVLI.....H
PsChR FMFPGLFLAGPEGTNALSWAGSTIGHTVADLLSKNAWGMIGHFLRLEI.....H
TsChR FMFPGLFLAGPEGTQALSWAGTTIGHTVADLLSKNAWGMIGHFLRVEI.....H
CrChR1 AMFPVLFLLGPEGFGHINQFNSAIAHAILDLASKNAWSMMGHFLRVKI.....H
CrChR2 GMFPILFILGPEGFGVLSVYGSTVGHTIIDLMSKNCWGLLGHYLRVLI.....H
VcChR1 GMFPVLFLLGTEGFGHISPYGSAIGHSILDLIAKNMWGVLGNYLRVKI.....H
VcChR2 GMFPVLFLLGPEGFGHLSVYGSTIGHTIIDLLSKNCWGLLGHFLRLKI.....H
DsChR1 AMFPILFILGREGFGHITYFGSSIGHFILEIFSKNLWSLLGHGLRYRI.....R
MvChR1 LTFPGWFLLGPEGLEVVTGTVSTLMHACSDLISKNLWGFMDWHLRVLVARHHRKLFKAEE
CyChR1 SFFPLIFLFGQSGFKKISPYADVIASSFGDLISKNAFGMLGHFLRVKI.....H
CaChR1 SFFPLIFLFGQSGFKKISPYADVIASSFGDLISKNMFGLLGHFLRVKI.....H
β5
β6
C1C2GA
320
330
340
C1C2GA EHILIHGDI......RK..TTKL.NIGGTEIEVETL.....V....EDEAEAGAV.....
PsChR KHIIIHGDV......RRPITVN..TL...GREV.TV..SCFVDKEEEEDE.DERISTKTYA
TsChR KHIIIHGDV......RRPVTVKALGR...QVSVNCF...VDKEEEEEDE.RI.........
CrChR1 EHILLYGDI......RK..KQKV.NVAGQEMEVETM.....V..HEEDDE..........
CrChR2 EHILIHGDI......RK..TTKL.NIGGTEIEVETL.....V....EDE.AEAGAVP...
VcChR1 EHILLYGDI......RK..KQKI.TIAGQEMEVETL.....V...AEEE.D.........
VcChR2 EHILLYGDI......RK..VQKI.RVAGEELEVETL.....M....TEE.APDTVKKSTA
DsChR1 QHIIIHGNL......TK..KNKI...NIAGDNVEVE.....E...................
MvChR1 EHALKKGQTLEPGMPRS..TSFV.RGLGDDVEIDPSYELYRLKRQNHPEYFL........
CyChR1 EHILKHGDI......RK..TTHL.RIAGEEKEVETF.....V....EEE...........
CaChR1 EHILKHGDI......RK..TTHL.RIAGEEKEVETF.....V....EEEDEDTVKHSTKE
C1C2GA
C1C2GA ....
PsChR NRASFMKMRNDMEQRGIQTRKSLEMLAPPPALNDGSIVLAVADPMTLTFF
TsChR ....
CrChR1 ....
CrChR2 ....
VcChR1 ....
VcChR2 QYANRESFLTMRDKLKEKGFEVRASLDNSGIDAVINHNNNYNNALAN...
DsChR1 ....
MvChR1 ....
CyChR1 ....
CaChR1 LANRGSFIVMRGNMKAQGIDVRASLDMEEDEEGGMGKGKGKGAG......

Supplementary Figure 13: Sequence alignment. Shown are C1C2GA, ChR from *Platymonas subcordiformis* (PsChR, GenBank ID: AGF84747.1), ChR from *Tetraselmis striata* (TsChR, GenBank ID: AHH02155.1), ChR1 from *Chlamydomonas reinhardtii* (CrChR1, GenBank ID: 15811379), ChR2 from *Chlamydomonas reinhardtii* (CrChR2, GenBank ID: 158280944), ChR1 from *Volvox carteri* (VcChR1, UniProtKB ID: B4Y103), ChR2 from *Volvox carteri* (VcChR2, UniProtKB ID: B4Y105), ChR1 from *Dunaliella salina* (DsChR1, GenBank ID: AEY68833.1), ChR1 from *Mesostigma viride* (MvChR1, GenBank ID: 338176939), ChR1 from *Chlamydomonas yellowstonensis* (CyChR1, GenBank ID: AER58217.1), and ChR1 from *Chlamydomonas augustae,* (CaChR1, GenBank ID: AER58220.1). The C-termini are truncated. Secondary structure elements for C1C2 are shown as coils (α: α-helices, η: 3_{10}-helices) and arrows (β-strands). Identical and conservatively substituted residues are highlighted in red. The residues contributing to the putative Zn^{2+} binding site are colored cyan. The glycine at position 198 and the alanine at position 202 (in C1C2GA) are colored green.

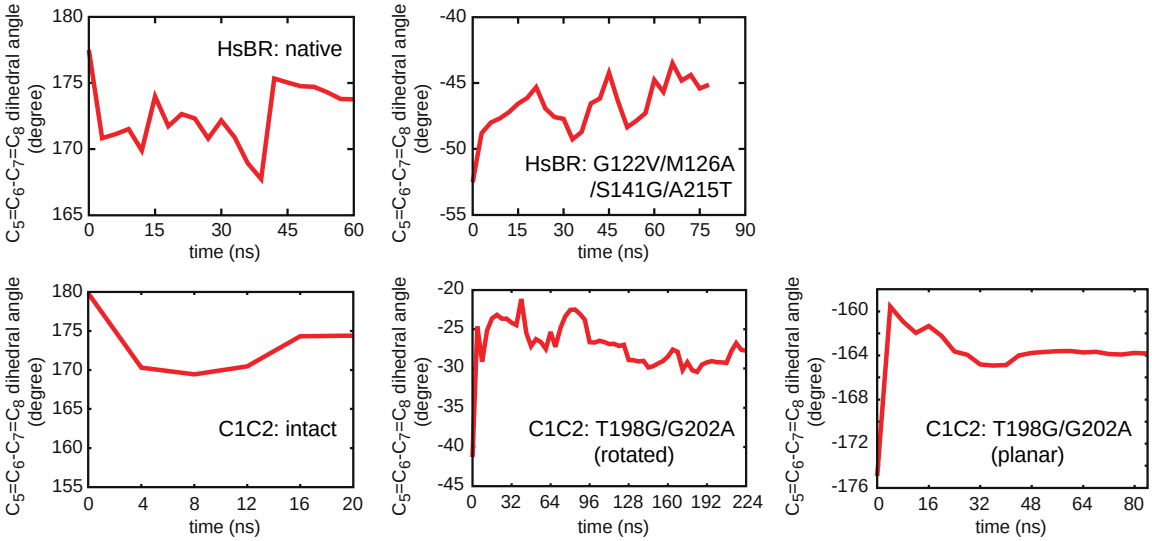

Supplementary Figure 14: Evolution of the dihedral angle around the C_5-C_6 bond in the RWFE free energy geometry optimization. Large changes of the dihedral angles and their convergence in the free energy geometry optimizations with MD trajectories for tens of nano-seconds were observed, indicating that the dihedral angles were well refined from the initial models without becoming trapped at a local minimum, which often occurs in a potential energy geometry optimization.

Supplementary Tables

Supplementary Table 1: Dihedral angles of C_5=C_6-C_7=C_8 in the structurally known rhodopsins.

	Dihedral angle of C_5-C_6-C_7-C_8 (°)
C1C2WT (PDB ID: 3UG9)	177.7
BR (PDB ID: 1C3W)	176.3
HR from *H. salinarum* (PDB ID: 1E12)	168.4
HR from *N. pharaonis* (PDB ID: 3A7K)	178.0
XR (PDB ID: 3DDL)	-179.3
SRII (PDB ID: 1H68)	178.0
Blue PR (PDB ID: 4JQ6)	-179.9
AR2 (PDB ID: 3AM6)	178.7
ASR (PDB ID: 1JGJ)	177.5
Archaerhodopsin-1 (PDB ID: 1UAZ)	-179.9
Archaerhodopsin-2 (PDB ID: 1VGO)	178.7
Bovine rhodopsin (PDB ID: 1F88)	-59.44
C1C2GA (this study)	-31.43

Supplementary Table 2: Torsional angles of C_5=C_6-C_7=C_8 of RPSB in the computational models (degrees).

C1C2		HsBR	
intact	T198G/G202A	native	M118A/G122A/S141G/A215T[b]
174.4	-27.7 (-163.9[a])	173.8	-45.1

[a] 6-*s*-*trans* conformation.

[b] Mutations in HsBR corresponding to the M128A/G132A/S151G/A225T mutations in AR3.

Supplementary Table 3: Fitting parameters of decomposition of absorption spectra of C1C2WT and C1C2GA shown in Supplementary Fig. 3[a].

C1C2WT: three Gaussian functions			
n	a_n	b_n / (kcal/mol)$^{-2}$	c_n / kcal/mol
1	0.567	0.0793	58.7
2	0.503	0.0547	63.4
3	0.449	0.00512	71.5
C1C2WT: three Gaussian functions assuming the same widths for the main and shoulder peaks			
n	a_n	b_n / (kcal/mol)$^{-2}$	c_n / kcal/mol
1	0.680	0.0670	59.0
2	0.431		64.1
3	0.453	0.00582	71.5
C1C2WT: two Gaussian functions			
n	a_n	b_n / (kcal/mol)$^{-2}$	c_n / kcal/mol
1	0.859	0.0318	60.7
2	0.464	0.00894	71.4
C1C2GA: two Gaussian functions			
n	a_n	b_n / (kcal/mol)$^{-2}$	c_n / kcal/mol
1	0.750	0.0247	62.4
2	0.498	0.00720	72.1
C1C2GA: three Gaussian functions			
n	a_n	b_n / (kcal/mol)$^{-2}$	c_n / kcal/mol
1	0.590	0.0181	66.8
2	0.585	0.0365	60.9
3	0.324	0.00544	80.7
C1C2GA: three Gaussian functions assuming the same widths for two peaks			
n	a_n	b_n / (kcal/mol)$^{-2}$	c_n / kcal/mol
1	0.407	0.0298	69.3

2	0.867		61.8
3	0.338	0.00628	80.0

[a] The absorption intensity $g(x)$ is fitted by Gaussian functions $g(x) = \sum_n a_n \exp(-b_n(x - c_n)^2)$, where x is the absorption energy in kcal/mol.

Supplementary Table 4: Absorption maximum, opsin shift and retinal configuration of wild type (WT) AR3 and various mutants.

Opsin type	λ_{max} [nm]	$\Delta\upsilon$ [cm^{-1}]	$\Delta\Delta\upsilon$ [cm^{-1}][b]	all-*trans* [%][c]
WT	552[a]	-	-	53 ± 2[a]
M128A	536[a]	541[a]	-	68 ± 1[a]
G132V	526	895	-	65 ± 3
A225T	540	403	-	70 ± 2
M128A/G132V	471	3115	1679	75 ± 3
M128A/S151G	505	1686	ND	51 ± 3
M128A/A225T	518	1189	245	51 ± 3
G132V/A225T	508	1569	271	75 ± 2
M128A/S151G/A225T	505	1686	-403	41 ± 2
M128A/S151A/A225T	491	2251	ND	71 ± 2
M128A/G132V/A225T	454	3910	2071	65 ± 3
M128A/G132A/S151G/A225T	471	3115	ND	51 ± 3
M128A/G132V/S151G/A225T	461	3576	-324	70 ± 1

ND: not determined.

[a] From Sudo et al. (2013) J. Biol. Chem.

[b] Differences between the spectral shift of the mutant and the sum of the shifts of the mutants with fewer replacements, indicating the synergetic effect of the spectral shift.

[c] The molar composition of each retinal isomer was calculated from the areas of the peaks in the HPLC patterns.

Supplementary Table 5. Absorption maximum, opsin shift, and retinal configuration of WT and various mutants of HwBR and GR.

Opsin type	λ_{max} [nm]	$\Delta\upsilon$ [cm^{-1}]	all-*trans* [%] [b]
(HwBR)-WT	552[a]	-	79 ± 2[a]
M126A/G130V	487	2418	75 ± 3
M126A/G130V/A223T	472	3070	70 ± 1
(GR)-WT	540	-	90 ± 3
M158A	535	173	72 ± 2
G162V	504	1323	93 ± 2
M158A/G162V	498	1562	93 ± 3
M158A/G162V/A256T	474	2579	64 ± 2

[a] From Sudo et al. (2013) J. Biol. Chem.

[b] The molar composition of each retinal isomer was calculated from the areas of the peaks in the HPLC patterns.